



OPEN Two dynamical models for male infertility and their stability and sensitivity analysis

Somaye Ghiasi Hafezi¹, Mahdi Ranjbar^{2✉}, Atena Ghasemabadi⁴, Sohrab Effati^{2,3✉}, Alvand Naserghandi⁵, Kosar Namakin⁶ & Farzad Allameh⁵

Mathematical models can estimate the success rate of assisted reproductive technology (ART) and determine which treatment suits the best. In this study, the authors introduce two new dynamic models that can predict the success rate of ART models for each individual based on the etiology of their infertility, clinical findings, and lab tests. The study shows that the equilibrium point free of disease is asymptotically stable and forward bifurcation occurs. Our dynamical models evaluate ART success rates in our subgroups considering couples under Intrauterine insemination (IUI), In Vitro Fertilization–Embryo Transfer (IVF), Intra–Cytoplasmic Sperm Injection (ICSI) treatment methods. Sensitivity analysis of parameters suggests that an increase in infertile couples who use IUI and ICSI treatment methods can result in better disease control and a more favorable outcome. It should be noted that the proposed models provide a systematic framework for simulating the dynamics of infertility and assessing the effectiveness of various ART. From a clinical perspective, these models have the potential to enhance decision-making by predicting the probability of ART success under diverse treatment scenarios. Such predictions may facilitate the personalization of treatment strategies based on individual patient profiles and contribute to more efficient resource allocation and planning within fertility centers.

Keywords Male infertility, Dynamical models, Asymptotically stable, Forward bifurcation

Modelling and mathematics has always gained from its involvement with developing sciences. Biomedical science is clearly the premier science of the foreseeable future. Therefore mathematicians must become involved with biology¹. It is well understood that mathematical, data mining, and statistical modeling and analysis are the keys to future breakthroughs in areas including the understanding of biological systems, the treatment of diseases, drug development, and targeted clinical trials. This is due to the fact that those enable us to come up with experiments that are both useful and efficient, uncover trends in data, and develop models that help in predicting and, hence, controlling the future outcomes.

The most common application of mathematics in medicine and pharmacology are machine learning and statistics. This manuscript prioritizes mathematical modeling over machine learning and statistical approaches, as it offers transparent, dynamic, and actionable insights that are essential for clinical decision-making. In contrast, machine learning methods for pattern recognition typically require large datasets, and statistical models often fail to capture the dynamic interactions among multiple factors. Indeed, the studies of mathematical modeling play a considerable role in analyzing the factors that may affect the spreading of the disease (see^{2–8}). In this regard, dynamic models that are closer to reality are less commonly used. In a typical traditional approach, data are phenomenologically analyzed by applying a regression model consisting of merely observed variables, not deeply considering the mechanism lying behind them. In contrast, in a dynamical model, we incorporate variables of the number of susceptible individuals that are not available or at least very difficult to obtain. Also, dynamic models are invaluable because they allow us to examine relationships that could not be sorted out by purely experimental methods and to make forecasts that cannot be made strictly by extrapolating from data. They are often used to the mathematical modeling of infectious diseases⁹, Ross and Hudson^{10,11}, Kermack and McKendrick¹², and Kendall¹³.

¹Biostatistics School of Health, Mashhad University of Medical Sciences, Mashhad, Iran. ²Department of Applied Mathematics, Faculty of Mathematical Science, Ferdowsi University of Mashhad, Mashhad, Iran. ³Center of Excellence of Soft Computing and Intelligent Information Processing (SCIIP), Ferdowsi University of Mashhad, Mashhad, Iran. ⁴Esfarayan University of Technology, Esfarayan, North Khorasan, Iran. ⁵Men's Health & Reproductive Health Research Center, Shahid Beheshti University of Medical Sciences, Tehran, Iran. ⁶Student Research Committee, Shahid Beheshti University of Medical Sciences, Tehran, Iran. ✉email: mahdi.ranjbar@um.ac.ir; s-effati@um.ac.ir

Accordingly, mathematical modeling can play a crucial role in advancing our understanding of male infertility and optimizing assisted reproductive technology (ART) outcomes. Given the multifactorial nature of male infertility, traditional statistical models often fall short in capturing the dynamic interactions between clinical, hormonal, and genetic factors influencing reproductive success. In this study, we propose two novel dynamic models that integrate these complexities to more accurately predict ART success rates. These models provide a framework for assessing the impact of various infertility treatments, including Intrauterine Insemination (IUI), In Vitro Fertilization-Embryo Transfer (IVF), and Intra-Cytoplasmic Sperm Injection (ICSI), on patient outcomes. By incorporating sensitivity analysis and stability evaluation, our approach offers a more systematic method for identifying key parameters that affect treatment efficacy. The application of mathematical models in reproductive medicine is essential for refining treatment strategies, minimizing trial-and-error approaches, and ultimately improving clinical decision-making for couples undergoing ART. The primary aim of this study is to develop and analyze these models for male infertility, with the objective of accurately predicting ART success rates and supporting clinical decision-making in treatment planning. We hypothesize that dynamic modeling of the underlying biological processes can enhance predictive accuracy and inform clinical strategies. Through sensitivity analysis and model validation, we aim to evaluate the practical utility of these models in real-world fertility treatment scenarios. The first model presented in this study analyzes the dynamics of infertility treatment in couples with mild oligospermia and severe male factor infertility. The second model, developed specifically for male infertility, introduces a more comprehensive framework that accounts for sperm sampling methods in infertile couples. These models assess ART success rates in defined subgroups by considering the effectiveness of IUI, IVF, and ICSI treatment methods.

Infertility is a multifactorial disease affecting about 50 million couples worldwide; in half of the cases, a male factor contributes to or is solely responsible for the failure to conceive¹⁴. Male infertility can be classified into four major etiological groups¹⁵.

1. Hypothalamic pituitary axis dysfunction.
2. Quantitative alterations of spermatogenesis.
3. Qualitative alterations of spermatogenesis.
4. Ductal obstruction/ dysfunction.

There are many known origins linked to male infertility, such as age, stress, individual genetics, lifestyle (obesity, smoking, and alcohol), immunological disorders, environmental factors, and other causes congenital or acquired urogenital dysfunctions, varicocele, endocrine imbalance and infections^{16,17}. Semen analysis is the cornerstone for laboratory evaluation of male infertility and plays a vital role in understanding the cause of infertility¹⁸. Importantly, it emphasizes that semen analysis alone cannot predict fertility because the couple's fertility potential determines whether they are fertile or infertile. However, it does not reduce the fundamental role of semen analysis¹⁹. Semen analysis results cannot accurately predict fertility, and men with seemingly low-quality semen samples can still achieve pregnancy²⁰. The fertility potential of the couple determines the likelihood of conceiving, and a higher motile sperm count increases the chances of pregnancy but does not guarantee it. As, fertile men have been found to have low sperm counts, and men with oligospermia can still achieve pregnancy without ART²¹. It reflects the production of spermatozoa in the testes, the patency of the duct system, and the glandular secretory activity²². The total number of spermatozoa per ejaculate and the sperm concentration is associated with fertility outcomes, such as conception, time to pregnancy, and pregnancy rates²³. As a diagnostic test, conventional semen analysis allows for the detection of absolute cases of male infertility, such as oligospermia, azoospermia, and teratospermia. Based on this, absolute cases of male infertility such as oligospermia (mild: 10-15 million sperm per ml, moderate: 5 to 10 million sperm per ml, and severe: less than 5 million sperm per ml), azoospermia (complete absence of sperm)²⁴, and teratospermia (higher ratio of morphologically abnormal sperm) are diagnosed²⁵. Azoospermia or oligospermia due to disruption of spermatogenesis are common causes of human male infertility²⁶.

Management and specific treatment methods for the causes of male infertility are less evaluated than female infertility. Despite this gap, there are still several proven methods that can optimize male fertility potential²⁷. The basic foundation of the treatments of male infertility is the lifestyle of men, and they continue with medical treatments and then surgery. All of these treatments aim to improve male fertility potential by improving Total Motile Sperm Count, which can improve all aspects of male reproduction, including IVF and ICSI²⁸. However, as a next step when treatments are not effective, ART programs may be recommended. Various factors are involved in the decision to perform ART, including the degree of impairment in the couple's conception potential (mother's age, ovarian reserve, cause of infertility), sexual function and duration of infertility. They should be done jointly by gynecologists and andrologists²⁹. IUI is often the first ART performed an infertile couple³⁰. Indications of using IUI are based on erectile dysfunction or other sexual or ejaculatory dysfunction, Mild to moderate seminal alteration (not otherwise treatable or failed treatment), Sexually transmitted diseases (i.e., HIV), and Idiopathic infertility (normozoospermia)³¹. IVF is used for the treatment of male infertility in patients with moderate oligospermia. However, in severe oligospermia and poor sperm motility, the fertilization rate of the oocytes is much less³². On the other hand, after an IUI failure, IVF Could be our choice. ICSI has revolutionized the treatment and improved the prognosis for infertile men with very severe oligospermia³³.

Obstructive and non-obstructive azoospermia (testicular or epididymal sperm), Immotile sperm Antisperm antibodies, Necrozoospermia, and Globozoospermia are the other indications for ICSI³⁴. IUI as a first-line strategy in cases of unexplained and mild/moderate male infertility remains controversial. In conclusion, it is vital to determine which method suits the best for the infertile couple. Although the male factor seems to be less critical than the female one, it is still preferable to improve spermatogenesis before launching the IVF process, carefully anticipating the true ameliorative potentials of any treatment and determining the "window of time

available” to achieve this goal by prioritizing maternal age and ovarian reserve as more important factors^{35,36}. Finally, confounding variables such as age, reproductive history, length of infertility, and lifestyle can influence the results of IVF treatment. These variables should all be taken into account for an accurate prediction of IVF effectiveness.^{37,38}

In this paper, two new dynamical models of male factor infertility are introduced. The inclusion criteria include couples suffering infertility due to mild or severe male factors, and those who did not meet these criteria were excluded. Based on this goal, the study was performed on the records for IVF, IUI, and ICSI treatments.

Methods

Dynamical models are simplified representations of some real-world entity in equations. These models are called dynamic because they describe how system properties change over time. Since mathematical modeling is needed to understand the dynamics of diseases, many studies in biology or medicine use them. In this paper, two dynamic models for describing couples’ infertility focusing on men’s causes are considered.

First model formulation and its analysis

In this model, the population is divided into six groups as follows:

1. Susceptible (S) persons include those couples who have just been referred to the clinic but whose illness has not been confirmed.
2. Infertile couples (I) are those who have visited the doctor and taken preliminary tests, and the cause of infertility has been diagnosed as being related to men.
3. People who are under treatment using IUI (T_1).
4. People who have received IVF treatment (T_2).
5. People who have undergone testicle biopsy using ICSI (T_3).
6. Couples who have received treatment and become fertile (R).

The proposed model consists of seven equations. The first two equations of the model show a susceptible-infected (SI) model. The next three equations of the model denote the treatment model (T) of infertile people. Finally, the sixth equation shows the recovered model (R). Based on, the first model is named a basic SITR model for infertile couples. The mathematical model of this biological phenomenon is designed in the following form:

$$\left\{ \begin{array}{l} \frac{dS}{dt} = L - \alpha S - \beta(\delta_1 T_1 + \delta_2 T_2)S, \\ \frac{dI}{dt} = \beta(\delta_1 T_1 + \delta_2 T_2)S - (\eta_1 + \eta_2 + \eta_3 + \alpha)I, \\ \frac{dT_1}{dt} = \eta_1 I - (\delta_1 + \alpha)T_1, \\ \frac{dT_2}{dt} = \eta_2 I + kh\delta_1 T_1 - (\alpha + (r_1 + r_2)\delta_2)T_2, \\ \frac{dT_3}{dt} = \eta_3 I + (1 - k)h\delta_1 T_1 + r_2\delta_2 T_2 - (\delta_3 + \alpha)T_3, \\ \frac{dR}{dt} = (1 - h)\delta_1 T_1 + r_1\delta_2 T_2 + u\delta_3 T_3 - \alpha R, \\ \frac{dN}{dt} = L - \alpha N - (1 - u)\delta_3 T_3. \end{array} \right. \quad (1)$$

Table 1 provides descriptions and ratio values of the parameters of the first dynamical model, which are obtained according to the data of the problem per day. The parameters in the model are derived from clinical studies and population-level data on infertility and ART success rates for both mild and severe oligospermia. Below, we provide a detailed explanation of the key parameters and their biological rationale:

1. Rate of death (α): This parameter accounts for couples who discontinue treatment without achieving pregnancy or who experience natural mortality. The values of α are based on dropout rates observed in ART clinics and general population mortality rates³⁹.
2. Rate of birth (L): This parameter represents the rate at which new couples seek infertility evaluation. The values are estimated from demographic data on infertility prevalence and referral rates to fertility clinics²⁷.
3. Rate of illness return (β): This parameter reflects the probability of infertility recurrence in couples with male factor infertility. The values are derived from longitudinal studies tracking infertility relapse following treatment⁴⁰.
4. Treatment rates ($\delta_1, \delta_2, \delta_3$): These parameters denote the rates at which couples undergo IUI, IVF, and ICSI treatments, respectively. The values are informed by clinical guidelines and ART success data.
5. Recovery rates (r_1, r_2): These parameters capture the success rates of IVF and ICSI treatments. The values are based on meta-analyses of ART outcomes⁴¹.
6. Transition probabilities (h, k, u): These parameters describe the likelihood of transitioning between treatment stages (e.g., from IUI to IVF or ICSI). The values are informed by clinical decision-making pathways in ART clinics⁴².

The architecture of the new dynamical model of the couples infertility with men’s causes is shown in Fig. 1.

Notation	Description of parameter	Mild oligospermia	Severe oligospermia
α	rate of death (the rate of couples who left the clinic without any results)	0.42	0.68
L	rate of birth (the rate of couples who have referred to the clinic)	0.45	0.07
β	The rate of the return of the illness in each couple with the men's causes	0.62	0.5
δ_1	The rate of treatment of people chosen for IUI treatment in time unit	0.035	0.016
δ_2	the rate of treatment of people chosen for IVF treatment in time unit	0.066	0.003
δ_3	The rate of treatment of people chosen for ICSI treatment in time unit	0.34	0.052
r_1	The rate of recovery in $\delta_2 T_2$	0.36	0
r_2	A fraction of $\delta_2 T_2$ who have got no result from IVF and hence, are under ICSI treatment	0.64	1
h	A percentage of $\delta_1 T_1$ who have received IVF in time t	0.85	0.84
$1 - h$	A percentage of $\delta_1 T_1$ who have received IUI and have recovered in time	0.15	0.16
k	A percentage of $h \delta_1 T_1$ who have entered T_2 treatment	0.12	0.27
$1 - k$	A percentage of $h \delta_1 T_1$ who have entered T_3 treatment	0.87	0.72
u	The percentage of $\delta_3 T_3$ who have received ICSI treatment and have recovered in time t	0.29	0.06
$1 - u$	A fraction of $\delta_3 T_3$ who have not become fertile due to menopause, Azoospermia or old age and have left the treatment	0.71	0.93
η_1	The percentage of I who have received IUI treatment in time t .	0.07	0.22
η_2	The percentage of I who have received IVF treatment in time t	0.14	0.05
η_3	The percentage of I who have received ICSI treatment in time t	0.75	0.73

Table 1. Description and ratio values of the parameters in the first dynamical model.

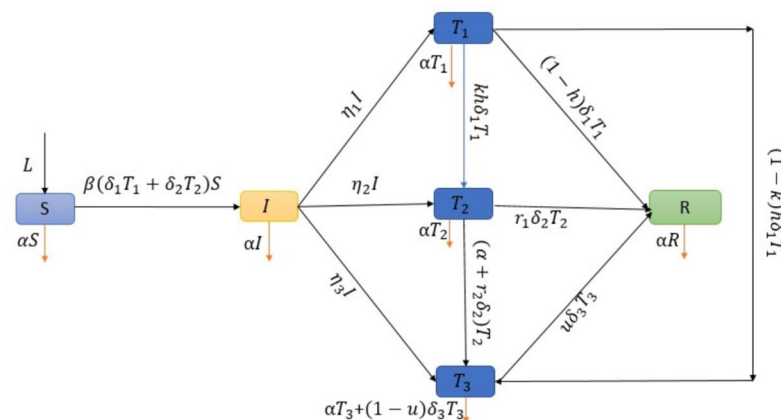


Fig. 1. Architecture of the first model for men's infertility.

Stability of the first model

Regarding the biological hypotheses of the first model, the investigation space of the model is as follows:

$$E = \{(S, I, T_1, T_2, T_3, N) \mid 0 \leq S + I + T_1 + T_2 + T_3 \leq N\}.$$

In this model, the basic reproductive number R_0 is shown with R_{B_0} . There is a tendency to calculate R_{B_0} , which is the number of secondary patients who have returned to the illness during the illness period⁴³. The R_{B_0} is got by using the next generation matrix as follows:

$$R_{B_0} = \frac{\beta \delta_1 \eta_1 S_0}{a_{22} a_{33}} + \frac{\beta k h \eta_1 \delta_1 \delta_2 S_0}{a_{22} a_{33} a_{44}} + \frac{\beta \delta_2 \eta_2 S_0}{a_{22} a_{44}}, \quad (2)$$

where

$$a_{22} = \eta_1 + \eta_2 + \eta_3 + \alpha, \quad a_{33} = \delta_1 + \alpha, \quad a_{44} = \alpha + (r_1 + r_2) \delta_2.$$

To understand the system behavior, only variables S, I, T_1 and T_2 are used because the rest of the variables can be obtained by them. According to this, the Jacobin matrix in the equilibrium point free of disease $E_{B_0} = (S_0, 0, 0, 0)$ is considered as follows:

$$J_{B_0} = \begin{pmatrix} -\alpha & 0 & -\beta S_0 \delta_1 & -\beta S_0 \delta_2 \\ 0 & -a_{22} & \beta S_0 \delta_1 & \beta S_0 \delta_2 \\ 0 & \eta_1 & -a_{33} & 0 \\ 0 & \eta_2 & k h \delta_1 & -a_{44} \end{pmatrix}.$$

The famous threshold criterion then states that the disease can invade if $R_{B_0} > 1$, whereas it cannot if $R_{B_0} < 1$. Therefore, we have the following result.

Theorem 1 *The disease-free equilibrium point of the system (1) is asymptotically stable provided $R_{B_0} < 1$. If $R_{B_0} > 1$, then it is unstable.*

Proof The characteristic equation of matrix J_{B_0} is obtained as follows:

$$P_4(\lambda) = (\lambda + \alpha) \left(a_0 \lambda^3 + a_1 \lambda^2 + a_2 \lambda + a_3 \right),$$

where

$$\begin{aligned} a_0 &= 1, \\ a_1 &= a_{22} + a_{33} + a_{44}, \\ a_2 &= a_{33}a_{44} + (a_{22}a_{33} - \beta \delta_1 \eta_1 S_0) + (a_{22}a_{44} - \beta \delta_2 \eta_2 S_0), \\ a_3 &= (1 - R_{B_0})a_{22}a_{33}a_{44}. \end{aligned}$$

The eigenvalue $\lambda_1 = -\alpha < 0$. So it suffices to show that the roots of $(a_0 \lambda^3 + a_1 \lambda^2 + a_2 \lambda + a_3)$ are negative. Since it is difficult to determine the roots of this polynomial, by using the Lienard–Chipart rule as a stability criterion in Definition 1 of Appendix A, which is the result of Routh–Hurwitz stability criterion.

So we have to show $a_i > 0$ for $i = 1, 2, 3$ and $\Delta_2 > 0$. It is obvious $a_1 > 0$. Therefore, in the following, we first show that $a_2 > 0$. For this purpose, we use the assumption $R_{B_0} < 1$. According to this assumption and Eq. (2), we conclude that

$$\frac{\beta \delta_1 \eta_1 S_0}{a_{22}a_{33}} < 1 \implies a_{22}a_{33} - \beta \delta_1 \eta_1 S_0 > 0. \quad (3)$$

$$\frac{\beta \delta_2 \eta_2 S_0}{a_{22}a_{44}} < 1 \implies a_{22}a_{44} - \beta \delta_2 \eta_2 S_0 > 0. \quad (4)$$

Therefore, the inequality $a_2 > 0$ holds. Since $R_{B_0} < 1$, it follows $a_3 > 0$.

Finally, by using the Lienard–Chipart rule, it is enough to show $\Delta_2 = a_1 a_2 - a_3 a_0 > 0$. For this purpose, according to the definition of Δ_2 , we have

$$\begin{aligned} \Delta_2 &= \left(a_{22} + a_{33} + a_{44} \right) \left(a_{33}a_{44} + (a_{22}a_{33} - \beta \delta_1 \eta_1 S_0) \right. \\ &\quad \left. + (a_{22}a_{44} - \beta \delta_2 \eta_2 S_0) \right) + (R_{B_0} - 1). \end{aligned}$$

From (3), (4), and $R_{B_0} < 1$, one can conclude $\Delta_2 > 0$, and it completes the proof. \square

Forward bifurcation

Throughout the domain of dynamic modeling, the term forward bifurcation relates to a considerable change in the qualitative characteristics of a system, frequently arising from variations in the parameters of the model. Forward bifurcation relates to the occurrence of novel dynamics or changes in stability characteristics that can be initiated by modifications in the fundamental factors. This phenomenon holds significant importance in comprehending the behavior of complicated systems, specifically those that model biological processes.

Conversely, the concept of an equilibrium point free of disease within a dynamic model suggests a condition of stability wherein the system stays unimpacted by pathogenic factors or disruptions. Within the realm of health and disease, the equilibrium point indicates a situation in which the system, whether it relates to biology or other domains, achieves a state of equilibrium and optimal functioning, free of any adverse effects. The examination of these concepts within a dynamic model facilitates researchers in acquiring a more comprehensive understanding of how systems react to alterations, particularly in the realm of preserving well-being or comprehending the elements that contribute to the dynamics of diseases.

It can be shown that the system of the basic Sitr model has an endemic equilibrium point

$$E^{B*} = [s^{B*}, I^{B*}, T_1^{B*}, T_2^{B*}, T_3^{B*}, N^{B*}],$$

where

$$\begin{aligned} s^{B*} &= \frac{S_0}{R_{B0}}, \\ T_1^{B*} &= \frac{\eta_1 I^{B*}}{a_{33}}, \\ T_2^{B*} &= \left(\frac{\eta_2}{a_{44}} + \frac{kh\delta_1\eta_1}{a_{33}a_{44}} \right) I^{B*}, \\ T_3^{B*} &= \frac{I^{B*}}{a_{55}} \left(\eta_3 + \frac{1-kh\delta_1\eta_1}{a_{33}} + \frac{r_2\delta_2\eta_2}{a_{44}} + \frac{r_2\delta_2kh\delta_1\eta_1}{a_{33}a_{44}} \right), \\ N^{B*} &= \frac{a_{66}}{(1-u)\delta_3} T_3^{B*}, \\ I^{B*} &= \frac{LR_{B0}-\alpha S_0}{a_{22}R_{B0}}, \end{aligned}$$

In the following, we show that the forward bifurcation occurs for the first model.

Theorem 2 *The first model in the endemic equilibrium E^{B*} has a forward bifurcation.*

Proof From Equation $R_{B0} = 1$, the parameter β^* is obtained as follows:

$$\beta^* = \frac{a_{22}a_{33}a_{44}}{a_{44}\delta_1\eta_1 S_0 + kh\eta_1\delta_1\delta_2 S_0 + a_{33}\delta_2\eta_2 S_0}. \quad (5)$$

Now, one of the eigenvalues of the Jacobian matrix $J(E^{B*}, \beta^*)$ is $-\alpha$ and the other eigenvalues are the roots of the following polynomials:

$$a_0\lambda^3 + a_1\lambda^2 + a_2\lambda + a_3 = 0.$$

If $R_{B0} = 1$, then $a_3 = 0$, and Jacobian matrix has a eigenvalue equal to zero and the characteristic equation becomes as $\lambda^2 + a_1\lambda + a_2 = 0$.

Therefore zero is a simple eigenvalue of the Jacobian matrix $J(E^{B*}, \beta^*)$ and since a_1 and a_2 are positive all other eigenvalues of the Jacobian matrix $J(E^{B*}, \beta^*)$ have negative real parts. Therefore, condition (i) of Proposition 1 is satisfied.

Suppose that $w = (w_1, w_2, w_3, w_4)$ is a right eigenvector of the Jacobian matrix $J(E^{B*}, \beta^*)$ corresponding to the eigenvalue of zero. In this case, the right eigenvector $w = (w_1, \frac{a_{33}}{\eta_1}, 1, w_4)$ is gotten, where

$$\begin{aligned} w_1 &= \frac{-\beta\delta_1 s_0}{\alpha} - \frac{-\beta\delta_2 s_0}{\alpha} \left(\frac{\eta_2 a_{33}}{\eta_1 a_{44}} + \frac{kh\delta_1}{a_{44}} \right), \\ w_4 &= \frac{\eta_2 a_{33}}{\eta_1 a_{44}} + \frac{kh\delta_1}{a_{44}}. \end{aligned}$$

In the same way, if $v = (v_1, v_2, v_3, v_4)$ is left eigenvector of the Jacobian matrix $J(E^{B*}, \beta^*)$ corresponds to the eigenvalue of zero, then $v = (0, 1, v_3, v_4)$, where

$$v_3 = \frac{a_{22}a_{44}-\beta z}{\eta_1 a_{44}}, \quad v_4 = \frac{\beta\delta_2 s_0}{a_{44}}.$$

According to the values of w and v , we get

$$\begin{aligned} a &= \sum_{k,i,j=1}^n v_k w_i w_j \frac{\partial^2 F_k}{\partial x_i \partial x_j}(0, 0) \\ &= \beta^{B*} (\delta_1 w_1 + \delta_2 w_1 w_4) < 0, \\ b &= \sum_{k,i=1}^n v_k w_i \frac{\partial^2 F_k}{\partial x_i \partial \phi}(0, 0) = s_0 (\delta_1 + \delta_2 w_4) > 0. \end{aligned}$$

Therefore, according to the case (d) of Proposition 1 in Appendix A, the system has a forward bifurcation. \square

Second model formulation and its analysis

Considering the details, a more complete form of the proposed model for male infertility can be introduced. In this model, in addition to considering the assumptions of the first model, sperm sampling of infertile couples is also considered. Sperm sampling of these individuals is done by three methods: Ejaculation (K_1), testicular sperm extraction (TESE) (K_2), and microscopic testicular sperm extraction (micro TESE) (K_3).

The proposed model consists of ten equations. The first five equations of the model show an SI model. The next three equations of the model denote the treatment model (T) of infertile people. Finally, the ninth equation also shows the recovered model (R). This model is named a complementary Sitr model that is a developed form of the basic Sitr model. The dynamical model of this biological phenomenon is designed as follows:

$$\left\{ \begin{array}{l} \frac{dS}{dt} = L - \alpha S - \beta(\delta_1 T_1 + \delta_2 T_2)S, \\ \frac{dI}{dt} = \beta(\delta_1 T_1 + \delta_2 T_2)S - (\nu_1 + \nu_2 + \nu_3 + \alpha)I, \\ \frac{dK_1}{dt} = \nu_1 I - (\eta_1 + \eta_2 + \eta_3 + \alpha)K_1, \\ \frac{dK_2}{dt} = \nu_2 I - (\eta_4 + \eta_5 + \alpha)K_2, \\ \frac{dK_3}{dt} = \nu_3 I - (\eta_6 + \eta_7 + \alpha)K_3, \\ \frac{dT_1}{dt} = \eta_1 K_1 - (\delta_1 + \alpha)T_1, \\ \frac{dT_2}{dt} = \eta_2 K_1 + \eta_4 K_2 + \eta_6 K_3 + kh\delta_1 T_1 \\ \quad - ((r_1 + r_2)\delta_2 + \alpha)T_2, \\ \frac{dT_3}{dt} = \eta_3 K_1 + \eta_5 K_2 + \eta_7 K_3 + r_2\delta_2 T_2 + (1 - k)h\delta_1 T_1 \\ \quad - (\delta_3 + \alpha)T_3, \\ \frac{dR}{dt} = (1 - h)\delta_1 T_1 + r_1\delta_2 T_2 + u_3\delta_3 T_3 - \alpha R, \\ \frac{dN}{dt} = L - \alpha N - (1 - u_3)\delta_3 T_3. \end{array} \right. \quad (6)$$

Table 2 provides descriptions and ratio values of the parameters in the second dynamic model, which are obtained according to the data of the problem per day.

The architecture of the second model of the couples's infertility with men's causes described by Eq. (6), is shown in Fig. 2.

Stability of the second model

Similar to the first Sitr model, the linearization matrix of the second Sitr model at an equilibrium point is as follows:

$$J_{C0} = \begin{pmatrix} -\alpha & 0 & 0 & 0 & 0 & -\beta S_0 \delta_1 & -\beta S_0 \delta_2 \\ 0 & -b_{22} & 0 & 0 & 0 & \beta S_0 \delta_1 & \beta S_0 \delta_2 \\ 0 & \gamma_1 & -b_{33} & 0 & 0 & 0 & 0 \\ 0 & \gamma_2 & 0 & -b_{44} & 0 & 0 & 0 \\ 0 & \gamma_3 & 0 & 0 & -b_{55} & 0 & 0 \\ 0 & 0 & \eta_1 & 0 & 0 & -b_{66} & 0 \\ 0 & 0 & \eta_2 & \eta_4 & \eta_6 & kh\delta_1 & -b_{77} \end{pmatrix},$$

where

$$\begin{aligned} b_{22} &= \nu_1 + \nu_2 + \nu_3 + \alpha, & b_{33} &= \eta_1 + \eta_2 + \eta_3 + \alpha, \\ b_{44} &= \eta_4 + \eta_5 + \alpha, & b_{55} &= \eta_6 + \eta_7 + \alpha, \\ b_{66} &= \delta_1 + \alpha, & b_{77} &= (r_1 + r_2)\delta_2 + \alpha. \end{aligned}$$

In the second model, the basic reproductive number R_0 is shown by R_{C0} , which is obtained as follows:

$$\begin{aligned} R_{C0} &= \frac{\beta \delta_1 S_0 \eta_1 \nu_1}{b_{22} b_{33} b_{66}} + \frac{\beta \delta_1 \delta_2 S_0 kh \eta_1 \nu_1}{b_{22} b_{33} b_{66} b_{77}} + \frac{\beta \delta_2 S_0 \eta_2 \nu_1}{b_{22} b_{33} b_{77}} \\ &\quad + \frac{\beta \delta_2 S_0 \eta_4 \nu_2}{b_{22} b_{44} b_{77}} + \frac{\beta \delta_2 S_0 \eta_6 \nu_3}{b_{22} b_{55} b_{77}}. \end{aligned}$$

In this case, the disease can invade if $R_{C0} > 1$, whereas it cannot if $R_{C0} < 1$. Therefore, we have the following result.

Theorem 3 Let $E_{C0} = (S_0, 0, 0, 0, 0, 0, N_0)$ be the free equilibrium point of the second model. If $R_{C0} < 1$, then E_{C0} is asymptotically stable.

Proof The characteristic equation of matrix J_{C0} is obtained as follows:

$$P_7(\lambda) = (\lambda + \alpha) \left(\lambda^6 + b_1 \lambda^5 + b_2 \lambda^4 + b_3 \lambda^3 + b_4 \lambda^2 + b_5 \lambda + b_6 \right);$$

see the constants of b_i ($i = 1, \dots, 6$) in Appendix B. Since $\lambda_1 = -\alpha$ is one negative root of the characteristic equation, it suffices to show that the roots of

$$\lambda^6 + b_1 \lambda^5 + b_2 \lambda^4 + b_3 \lambda^3 + b_4 \lambda^2 + b_5 \lambda + b_6 = 0$$

Notation	Description of parameter	Mild oligospermia	Severe oligospermia
α	rate of death (the rate of couples who left the clinic without any results)	0.24	0.12
L	rate of birth (the rate of couples who have referred to the clinic)	0.4	
m_1	rate of death (the rate of I_1 who left the clinic without any results)	0.24	0.12
m_2	rate of death (the rate of I_2 who left the clinic without any results)	0.86	0.9
β	The rate of the return of the illness in each couple with the men's causes	0.4	0.2
δ_1	The rate of treatment of people chosen for IUI treatment in time unit	0.01	0.01
δ_2	the rate of treatment of people chosen for IVF treatment in time unit	0.18	0.005
δ_3	The rate of treatment of people chosen for ICSI treatment in time unit	0.8	0.9
ν_1	Rate of transmission from I to K_1	0.97	0.53
ν_2	Rate of transmission from I to K_2	0	0.08
ν_3	Rate of transmission from I to K_3	0.02	0.36
m_3	A fraction of K_1 who have left the clinic without any results	0.88	0.92
m_4	A fraction of K_2 who have left the clinic without any results	0.16	0.75
m_5	A fraction of K_3 who have left the clinic without any results	0.13	0.72
h	A percentage of $\delta_1 T_1$ who have received IVF in time t	0.84	0.83
$1 - h$	A percentage of $\delta_1 T_1$ who have received IUI and have recovered in time	0.15	0.16
k	A percentage of $h \delta_1 T_1$ who have entered T_2 treatment	0.11	0.014
$1 - k$	A percentage of $h \delta_1 T_1$ who have entered T_3 treatment	0.88	0.98
u_3	The percentage of $\delta_3 T_3$ who have received ICSI treatment and have recovered in time t	0.84	0.018
$1 - u_3$	A fraction of $\delta_3 T_3$ who have not become fertile due to menopause, Azoospermia or old age and have left the treatment	0.16	0.98
η_1	The percentage of K_1 who have received IUI treatment in time t	0.01	0.02
η_2	The percentage of K_1 who have received IVF treatment in time t	0.19	0.125
η_3	The percentage of K_1 who have received ICSI treatment in time t	0.83	0.029
η_4	The percentage of K_2 who have received IVF treatment in time t	0	0.0625
η_5	The percentage of K_2 who have received ICSI treatment in time t	0	0.096
η_6	The percentage of K_3 who have received IVF treatment in time t	0.114	1
η_7	The percentage of K_3 who have received ICSI treatment in time t	0.026	0.40
m_6	rate of death (the rate of T_1 who left the clinic without any results)	0.25	1
m_7	rate of death (the rate of T_2 who left the clinic without any results)	0.11	0.98
m_8	rate of death (the rate of T_3 who left the clinic without any results)	0.119	0.98
m_9	rate of death (the rate of who left the clinic without any results or die naturally)	0.25	0.127

Table 2. Description and ratio values of the parameters in the second dynamic model.

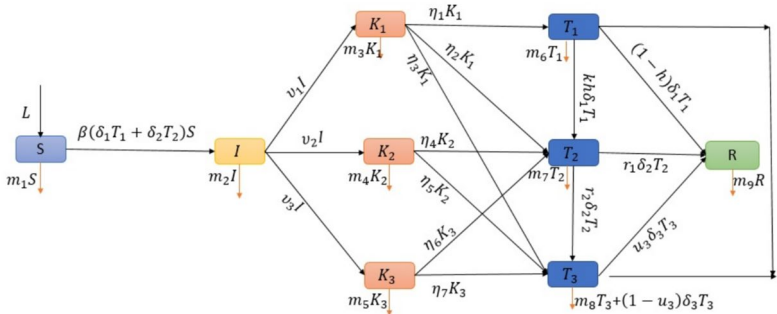


Fig. 2. Architecture of the second model for men's infertility.

are negative. Since it is difficult to determine the roots of this polynomial, we use the Lienard–Chipart rule as a stability criterion in Definition 1 of Appendix A, which is the result of Routh–Hurwitz stability criterion. So we have to show $b_i > 0$ for $i = 1, 2, 3, 4, 5, 6$ and $\Delta_1, \Delta_3, \Delta_5 > 0$. Since all parameters are positive, therefore $b_{jj} > 0$, for each $j \in \{1, 2, 3, 4, 5, 6, 7\}$. Also, according to $R_{C0} < 1$, we conclude that

$$\frac{\beta\delta_1 S_0 \eta_1 v_1}{b_{22} b_{33} b_{66}} < 1, \quad \frac{\beta\delta_1 \delta_2 S_0 k h \eta_1 v_1}{b_{22} b_{33} b_{66} b_{77}} < 1, \quad \frac{\beta\delta_2 S_0 \eta_2 v_1}{b_{22} b_{33} b_{77}} < 1,$$

$$\frac{\beta\delta_2 S_0 \eta_4 v_2}{b_{22} b_{44} b_{77}} < 1, \quad \frac{\beta\delta_2 S_0 \eta_6 v_3}{b_{22} b_{55} b_{77}} < 1.$$

According to the introduced assumptions, after simplifying the obtained expressions and arranging them, similar to Theorem 1, we showed that

$$b_0, b_1, b_2, b_3, b_4, b_5, b_6, \Delta_1, \Delta_3, \Delta_5 > 0,$$

and it completes the proof. \square

Forward bifurcation

In this section, we show that the system of the second model has an endemic equilibrium point as follows:

$$E^{C*} = [s^{C*}, I^{C*}, K_1^{C*}, K_2^{C*}, K_3^{C*}, T_1^{C*}, T_2^{C*}, T_3^{C*}]$$

see the components of E^{C*} , in Appendix C.

In the following, using Proposition 1 in Appendix A, the forward bifurcation occurs for the second model.

Theorem 4 *The second model in the endemic equilibrium E^{C*} has a forward bifurcation.*

Proof From equation $R_{C0} = 1$, the parameter β^* is obtained as follows:

$$\beta^* = \frac{b_{22} b_{33} b_{44} b_{55} b_{66} b_{77}}{E},$$

where

$$E = \beta\delta_1 s_0 \eta_1 v_1 b_{44} b_{55} b_{77} + \beta\delta_1 \delta_2 s_0 k h \eta_1 v_1 b_{44} b_{55} \\ + \beta\delta_2 s_0 \eta_2 v_1 b_{44} b_{55} b_{66} + \beta\delta_2 s_0 \eta_4 v_2 b_{33} b_{55} b_{66} \\ + \beta\delta_2 s_0 \eta_6 v_3 b_{33} b_{44} b_{66}.$$

Now, one of the eigenvalues of the Jacobian matrix $J(E^{C*}, \beta^*)$ is $-\alpha$, and the other eigenvalues are the roots of the polynomials $\lambda^5 + p_1 \lambda^4 + p_2 \lambda^3 + p_3 \lambda^2 + p_4 \lambda + p_5 = 0$; see the constants of p_i , ($i = 1, \dots, 5$) in Appendix D.

It can be shown that eigenvalues of the Jacobian matrix $J(E^{C*}, \beta^*)$ have negative real parts. Therefore, condition (i) of Proposition 1 is satisfied. Suppose that $w = (w_1, w_2, w_3, w_4, w_5, w_6, w_7)$ is a right eigenvector of the Jacobian matrix $J(E^{C*}, \beta^*)$ corresponding to the eigenvalue of zero. In this case, we have

$$w = (w_1, 1, \frac{\nu_1}{b_{33}}, \frac{\nu_2}{b_{44}}, \frac{\nu_3}{b_{55}}, \frac{\eta_1 v_1}{b_{33} b_{66}}, w_7),$$

where

$$w_1 = -\frac{\beta\delta_1 s_0 w_6 + \beta\delta_2 s_0 w_7}{\alpha},$$

$$w_7 = \frac{\delta_1 \eta_1 v_1}{\beta\delta_2 s_0} (b_{22} - \beta s_0).$$

If $v = (v_1, v_2, v_3, v_4, v_5, v_6, v_7)$ is a left eigenvector of the Jacobian matrix $J(E^{C*}, \beta^*)$ corresponding to the eigenvalue of zero, then the eigenvector is obtained as follows:

$$v = (0, \frac{b_{77}}{\beta\delta_2 s_0}, \frac{\eta_1 + \eta_2}{b_{33}}, \frac{\eta_4}{b_{44}}, \frac{\eta_6}{b_{55}}, 1, 1).$$

According to values of w and v , we get

$$\begin{aligned}
 a &= \sum_{k,i,j=1}^n v_k w_i w_j \frac{\partial^2 F_k}{\partial x_i \partial x_j}(0,0) \\
 &= \frac{-b_{77}}{\alpha \delta_2} \left(\frac{\eta_1 r_1 \delta_1}{b_{33} b_{66}} + \frac{\delta_1 \delta_2 \eta_1 r_1 (b_{22} - \beta s_0)}{\beta \delta_2 s_0} \right) \\
 &\quad \times \left(\frac{\eta_1 r_1 \beta \delta_1}{b_{33} b_{66}} + \delta_1 \eta_1 r_1 (b_{22} - \beta s_0) \right) < 0, \\
 b &= \sum_{k,i=1}^n v_k w_i \frac{\partial^2 F_k}{\partial x_i \partial \phi}(0,0) \\
 &= \frac{b_{77}}{\beta \delta_2} \left(\frac{\eta_1 r_1 \delta_1}{b_{33} b_{66}} + \frac{\delta_1 \eta_1 r_1 (b_{22} - \beta s_0)}{\beta s_0} \right) > 0.
 \end{aligned}$$

Therefore, according to the case (d) of Proposition 1 in Appendix A, the system has a forward bifurcation. \square

Data and statistical analysis

Data from 2474 cycles performed were collected. The data analyzed during the current study are not publicly available due to privacy and legal restrictions, but we confirm that all experimental protocols were approved by the Ethics Committee of Yazd University (Approval Number: IR.YAZD.REC.1401.019). Also, We confirm that all methods were carried out in accordance with relevant guidelines and regulations, and we emphasize that informed consent was obtained from all individuals participating or their legal guardian in this study.

We were selected only those couples for whom source of infertility were oligospermia and sever oligospermia. The collected demographic and clinical variables consist of infertility type (primary, secondary), women's ages, body mass index (BMI), infertility duration (years), type of ART, total number of retrieved oocytes, number of injected oocytes, number of embryos, number of transferred embryos, spermogram, maturation rate oocyte, fertilization rate after ICSI and data on embryo quality (grade A, grade B, and grade C).

The data's descriptive characteristics were presented using the mean (standard error) for continuous variables and frequency (percentage) for categorical variables. To compare the means of the variables across response categories, we employed the independent samples T-test after verifying the normality of the data distribution. Additionally, we utilized the chi-square test to evaluate the independence between categorical variables and the outcome. Among the assessed cycles, 1100 without spermogram (Data set 1 in Table 3) and 1374 with spermogram (Data set 2 in Table 3) were reported. Couples who were experiencing infertility caused by mild oligospermia or severe oligospermia were included as per the criteria, while those who did not meet these criteria were excluded from the study. Based on this goal, the study was performed on the records for IVF, IUI and ICSI including. The average rate of infertility subjects in with negative Beta human chorionic gonadotropin (Beta-HCG) sub-samples in Table 3 are significantly lower than the positive Beta-HCG (0.60 ± 0.27 vs. 0.72 ± 0.19 , p -value = 0.006) and (0.46 ± 0.26 vs. 0.58 ± 0.29 , p -value < 0.001) in mild oligospermia and sever oligospermia, respectively. A comparison was made between the quality of embryos in the mild oligospermia group, specifically in the positive and negative Beta-HCG groups. The results indicated a higher success rate in terms of embryo quality in the positive Beta-HCG group compared to the negative Beta-HCG group ($P = 0.007$). Table 3 lists the mean or frequency of the variables for both successful (positive Beta-HCG) and unsuccessful (negative Beta-HCG) data. The unadjusted results are shown using the T-test and chi-square test for continuous and categorical variables, respectively. Table 3 provides additional details of the patients' characteristics. It should be noted that in this paper the data set 1 is used for the results obtained in the first model and the data set 2 is used for the results obtained in the second model.

Results

Our dynamic models evaluate ART success rates in our subgroups considering IUI, IVF, and ICSI treatment methods. Furthermore, ICSI was more promising for male factors infertility. In all the methods of sperm collection, couples with mild oligospermia infertile use the ICSI method more than couples with severe oligospermia. The study shows that the disease-free equilibrium point is asymptotically stable, and that forward bifurcation occurs. The primary reproduction number must be reduced to less than one to eradicate the disease, which depends on the possibility of recovery. Sensitivity analysis of parameters suggests that an increase in infertile couples who use IUI and ICSI treatment methods can result in better disease control and a more favorable outcome.

In the first model, to check the possibility of our examination, to explain the dynamical conduct of the framework, we have directed numerical recreations with the assistance ode45 of MATLAB programming. Accompanying arrangement of parameter esteems are picked for simulation. Infertile couples are divided into two groups:

- i) infertility couples due to of mild oligospermia,
- ii) infertility couples due to of severe oligospermia.

Figs. 3 and 4 show the model simulations of infertility couples for mild oligospermia and severe oligospermia by the first model, respectively. For example, curve $R(t)$ in these figures show that the recovery rate in severe oligospermia is lower than in mild oligospermia or curve $T_3(t)$ show that the ICSI treatment method is more commonly used for treatment than the two other methods and the recovery rate in the ICSI method in the first

Data set 1: Among 1100 eligible participants without spermogram						
Variables	Mild Oligospermia	(n=499)	P-Value	Severe Oligospermia	(n=80)	P-Value
	Beta-HCG+ (n=143)	Beta-HCG- (n=365)		Beta-HCG+ (n=7)	Beta-HCG- (n=73)	
T_1 (IUI)	6(15.4%)	33(84.6%)		3(16.7%)	15(83.3%)	
T_2 (IVF)	27(42.9%)	46(57.1%)	0.090	0(0%)	4(100%)	0.360
T_3 (ICSI)	110(29.1%)	268(70.9%)		4(6.9%)	54(93.1%)	
Age	28.73 ± 4.55	29.58 ± 5.24	0.089	29.71 ± 8.97	33.22 ± 5.74	0.347
Rate of infertility	0.64 ± 0.22	0.68 ± 0.24	0.107	0.77 ± 0.20	0.85 ± 0.18	0.434
Maturation rate oocyte	0.84 ± 0.24	0.88 ± 0.37	0.527	1.45 ± 0.65	0.0.95 ± 0.55	0.088
BMI	26.16 ± 2.13	25.60 ± 2.72	0.637	24.33 ± 2.08	0.24.73 ± 3.53	0.854
Grade	A 52(42.3%)	71(57.7%)		1(8.3%)	11(91.7%)	
	B 70(28.1%)	179(71.9%)	0.007	2(7.1%)	26(92.9%)	0.931
	C 15(23.4%)	49(76.6%)		1(11.1%)	8(88.9%)	
Data set 2: Among 1374 eligible participants with spermogram						
Variables	Mild Oligospermia	(n=370)	P-Value	Severe Oligospermia	(n=183)	P-Value
	Beta-HCG+ (n=41)	Beta-HCG- (n=323)		Beta-HCG+ (n=18)	Beta-HCG- (n=165)	
T_1 (IUI)	0(0%)	4(100%)	-	0(0%)	2(100%)	-
T_2 (IVF)	41(12%)	330(88%)	0.74	18(9.9%)	163(90.1%)	0.74
T_3 (ICSI)	41(11.1%)	329(88.9%)	0.06	18(9.9%)	164(90.1%)	0.06
K_1 = Ejaculation	41(11.1%)	319(88.9%)		7(7.1%)	92(92.9%)	
K_2 = TESE	0(0%)	6(100%)	0.59	4(10.2%)	35(89.7%)	0.74
K_3 = Micro TESE	0(0%)	2(100%)		3(10.7%)	25(89.3%)	
Age	31.29 ± 5.23	31.08 ± 5.00	0.57	31.44 ± 4.55	30.21 ± 5.44	0.57
Rate of infertility	0.72 ± 0.19	0.60 ± 0.27	0.006	0.58 ± 0.29	0.46 ± 0.26	<0.001
Maturation rate oocyte	0.83 ± 0.15	0.86 ± 0.44	0.68	0.80 ± 0.17	0.83 ± 0.17	0.68
Grade	A 26(12.3%)	186(87.7%)		11(10.8%)	91(89.9%)	
	B 6(11.3%)	47(88.7%)	0.47	3(9.4%)	29(90.6%)	0.49
	C 0(0%)	3(100%)		0(0%)	4(100%)	

Table 3. Results of statistical analysis for continuous and categorical variables.

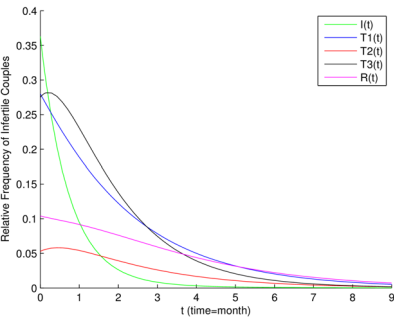


Fig. 3. Model simulations of infertility couples for mild oligospermia in the first model.

group is almost five times that of the second group. Also, curves of T_2 show the recovery rate in the IVF method for the first group is 36 times that of the second group.

The recovery rate in couples who use the IVF treatment is 36% in the first group and zero in the second group. That is, infertile couples in the second group are not treated with IVF at all (coefficient δ_2 in Table 1).

On the other hand, 64% of the couples in the first group do not benefit from IVF and chose the ICSI treatment method, and 100% of the couples in the second group do not get results from IVF and chose ICSI. Moreover, the couples in the second group are not treated with IVF at all (coefficient r_2 in Table 1).

Sensitivity parameters are those that have a significant impact on the dynamics of disease. Table 4 shows the sensitivity indices for parameters in the first model. The negative sensitivity index has an inverse proportional relationship with the basic reproduction number R_0 ; an increase in this parameter will bring about a decrease in the basic reproduction number R_0 . However, the size of the increase will be proportionally smaller than parameter β . If the sensitivity index is zero, it has no effect on disease control (fertility of couples).

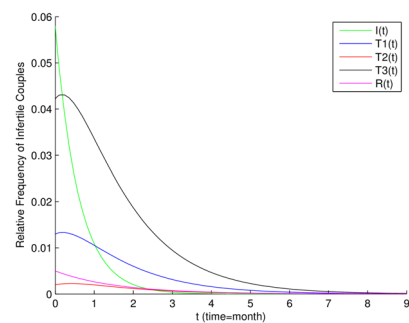


Fig. 4. Model simulations of infertility couples for severe oligospermia in the first model.

Parameters	Mild oligospermia	Severe oligospermia
β	1	1
δ_2	0.6740431795	0.04183941046
η_2	0.3461220993	0.1490679256
η_3	-0.6842239760	-0.4345238095
r_1	-0.03813158560	0
r_2	-0.06778948552	-0.0001845856344

Table 4. Sensitivity indices for parameters of the first model.

The positive sensitivity index has a directly proportional relationship with the basic reproduction number R_0 ; an increase in this parameter will bring about an increase in the basic reproduction number R_0 . However, the size of the increase will be proportionally smaller than parameter β . By increasing the recovery rate of couples who choose IVF (increasing δ_2) and decreasing the recovery rate of couples in $\delta_2 T_2$ (decreasing r_1), then the basic reproduction number R_0 will increase, and the number of infertile couples will increase. The sensitivity indices of δ_2 and η_2 are positive. Moreover, δ_2 is the rate of recovery for people chosen for IVF treatment, and η_2 is the percentage of infertile couples who have received IVF treatment. The sensitivity index of δ_2 is greater than the sensitivity index of η_2 . This means that the recovery rate, δ_2 , is a more effective parameter than receiving IVF treatment, η_2 , on couples' fertility.

In Table 4, the sensitivity indices of parameters show that the parameter β has the greatest impact on the value of R_0 , where β is the rate of the return of the disease in each couple. Specifically, if β increases, R_0 will also increase proportionally. Similarly, a decrease in β will result in a proportional decrease in R_0 . In other words, the relationship between β and R_0 is directly proportional. After the parameter β , the sensitivity index of η_3 has the most effect in controlling the disease. When the doctor has to choose the ICSI method for the infertile couple, it means that the severity of the disease in the infertile couple was high, and it was difficult to control the disease (fertility of couples).

The objective of infertile couples at the clinic is to address their infertility. Consequently, the key parameters doctors focus on are denoted as r_1 and r_2 . Also, r_1 represents the recovery rate for couples undergoing the IVF treatment method, while r_2 represents the recovery rate for couples utilizing the ICSI treatment method.

The sensitivity index of this model shows that prioritizing reducing the need for couples to return to the clinic is more beneficial than relying on any specific method of pregnancy assistance to treat infertile couples. Basically, it shows that prevention of frequent abortions is preferable to treatment in this field.

In the second model, Figs. 5–10 show predicted the evolution of infertile couples with two causes of infertility, mild oligospermia and severe oligospermia, for different sperm sampling of them.

The turquoise blue curve in Figs. 5–10 is increasing with mild oligospermia and almost constant in the severe oligospermia, and the number of recovered couples with the mild oligospermia is almost 2.5 times that of the severe oligospermia (see curve $R(t)$ in Figs. 5–10). Moreover, a comparison of the $K_2(t)$ and $K_3(t)$ curves reveals that TESE is more frequently utilized in cases of severe oligospermia during the first two months, whereas micro-TESE becomes the predominant method after the second month.

In Figs. 5 and 6, the IUI treatment method is considered. Couples with the mild oligospermia use spermography 1.8 times more than those with severe oligospermia (coefficient ν_1 in Table 2).

At the beginning of the period, the number of couples with the mild oligospermia who use IVF treatment is two times that of severe oligospermia (curve T_2 in Figs. 7 and 8). The recovery rate of IVF treatment for the mild oligospermia is almost 36 times that of severe oligospermia (coefficient δ_2 in Table 2). The slope of the curve $I(t)$ (the number of infertile couples) is higher in severe oligospermia than mild oligospermia. Thus, in the severe oligospermia group, the choice of treatment method and conclusion is faster than the mild oligospermia group.

The recovery rate in the mild oligospermia is 4.5 times that of severe oligospermia. The percentage of $\delta_3 T_3$, who have received ICSI treatment and have recovered, is 84% of the couples with the mild oligospermia and

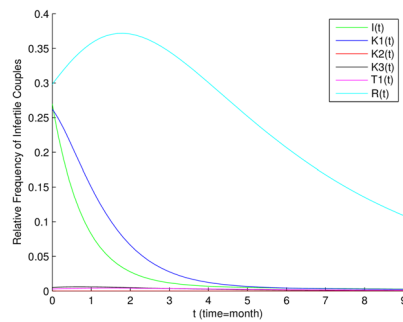


Fig. 5. Model simulations of infertility couples for the mild oligospermia with IUI treatment in the second model.

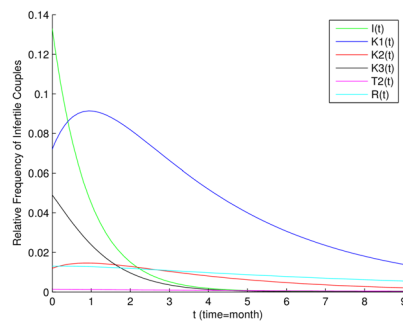


Fig. 6. Model simulations of infertility couples for the severe oligospermia with IUI treatment in the second model.

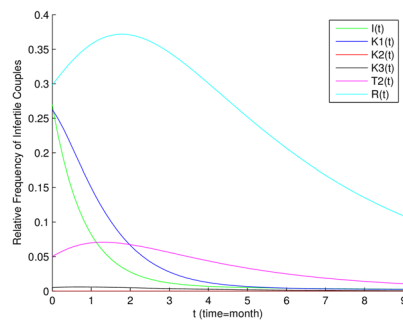


Fig. 7. Model simulations of infertility couples for the mild oligospermia with IVF treatment in the second model.

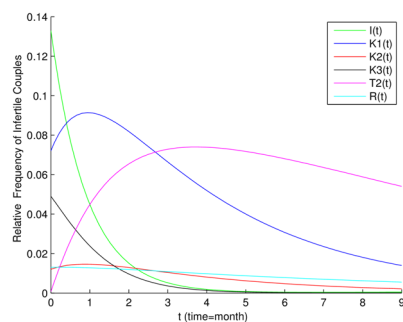


Fig. 8. Model simulations of infertility couples for the severe oligospermia with IVF treatment in the second model.

1.8% of the couples in severe oligospermia. That is, ICSI treatment was better with the mild oligospermia than in severe oligospermia (coefficient u_3 in Table 2).

The rate of transmission from infertile couples to the class of couples who use micro TESE testicular biopsy and ICSI treatment in the first group is lower than the second group (coefficient ν_3 in Table 2).

According to the results presented in Table 5, similar to the first model, the sensitivity index of the parameters is checked. Patients whose spermogram is TESE get better results than micro TESE, and more couples are fertilized. Parameters r_1 and r_2 are the rates of recovery in couples using the IVF and ICSI treatment method, respectively. Like the first model, prevention of repeated abortions is better than reusing contraceptive methods.

Discussion

It is important to note that these findings are derived from a theoretical mathematical framework and lack direct clinical validation. Mathematical models, by design, identify influential parameters but do not establish causal relationships. Therefore, these results should not be interpreted as definitive clinical recommendations. Nonetheless, the proposed models provide a structured framework for simulating infertility dynamics and evaluating the potential impact of various ART interventions. From a clinical perspective, these models may support decision-making by predicting the likelihood of ART success under different treatment scenarios, thereby assisting clinicians in tailoring treatment strategies to individual patients. Moreover, they may contribute to improved resource allocation and planning within fertility clinics.

This study presents a comprehensive analysis of two dynamic models related to male infertility, specifically focusing on oligospermia. Low sperm count, or oligospermia, is a common cause of male infertility and can significantly affect a couple's ability to conceive naturally. The findings derived from this investigation enhance the existing scholarly understanding of male infertility and potential methods for treatment. The success rates of ART techniques, namely IUI, IVF, and ICSI, were assessed using the proposed models. The findings indicated that ICSI demonstrated greater potential in addressing various etiologies associated with male factor infertility. Infertile couples diagnosed with oligospermia exhibited a higher tendency to use IVF and ICSI techniques compared to those with severe oligospermia. This observation aligns with previous research that has identified IVF and ICSI as often selected options for couples affected by oligospermia⁴⁴. Nevertheless, it is crucial to acknowledge that the selection of treatment options can be intricate and contingent upon several variables, such as the extent of oligospermia and the fertility potential of the female counterpart.

The study also showed that the equilibrium point free of disease exhibited asymptotic stability, and a forward bifurcation occurred. The findings from the sensitivity analysis indicate that an increase in the utilization of IUI and ICSI treatment procedures by infertile couples may lead to enhanced disease control and more favorable outcomes. It should be emphasized, however, that sensitivity analysis does not establish causal relationships. Instead, it serves as a tool to identify key parameters that significantly influence the outcomes of infertility treatments. Studies offer significant insights into the efficacy of ART techniques and the determinants that may impact their success rates. These results can provide valuable insights for healthcare professionals in making informed decisions on treatment options for couples experiencing infertility. Additionally, these findings may contribute to enhanced disease management strategies and ultimately lead to more positive outcomes. Nevertheless, further investigation is required to comprehensively understand the intricate interaction of variables that may impact the success rates of ART and to formulate more efficacious therapeutic approaches for couples experiencing infertility.

The first model in this study analyzed the dynamics of infertility treatment in couples with mild oligospermia and severe male factor infertility. The findings indicated that the percentage of successful pregnancies among couples who underwent IVF therapy was 36% in the first group, which consisted of individuals experiencing infertility caused by mild oligospermia. Conversely, the second group, comprising individuals with infertility attributed to severe oligospermia, exhibited a complete absence of successful conception. This finding suggests that the couples in the second group did not experience any positive effects from undergoing IVF therapy.

Parameters	Mild oligospermia	Severe oligospermia
β	1	1
δ_2	0.6853471285	0.3677797932
η_2	0.5957772792	-0.01686891733
η_3	-0.2675112095	-0.2094653346
η_4	0.01624929687	0.06930273377
η_5	-0.001015581055	-0.04554179647
η_6	0.002876328662	0.04786908195
η_7	0.002876328662	0.04786908195
ν_1	0.2665647987	0.2805208620
ν_2	-0.05626453384	-0.09103782274
ν_3	-0.03382967663	-0.07183598048
r_1	-0.005140103464	-0.0001532415805
r_2	-0.2415848629	-0.01501767489

Table 5. Sensitivity indices of parameters of the second model.

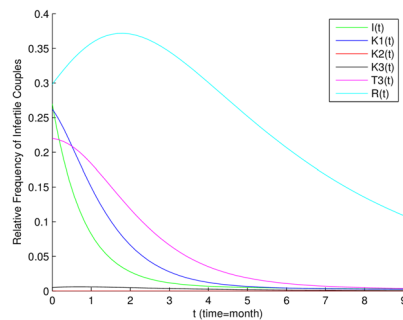


Fig. 9. Model simulations of infertility couples for the mild oligospermia with ICSI treatment in the second model.

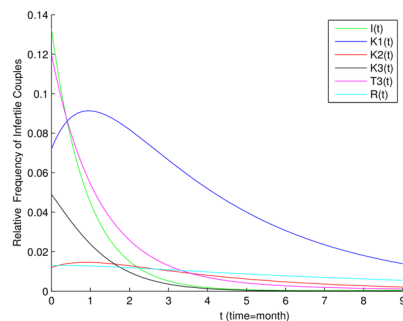


Fig. 10. Model simulations of infertility couples for the severe oligospermia with ICSI treatment in the second model.

Instead, they opted for ICSI as an alternate approach. Within the first group, a majority of 64% of the couples were unable to achieve favorable outcomes through IVF and subsequently chose to undergo ICSI treatment. Conversely, all couples in the second group exclusively pursued ICSI treatment. The observed recovery rate in the first group undergoing ICSI was about five times higher than that of the second group, indicating that ICSI may be a potentially more efficacious therapeutic alternative for couples experiencing severe oligospermia. To confirm these results, the success rates of IVF and ICSI in couples with severe male factor infertility exhibit variability across several research investigations^{45,46}. However, it is important to consider the complex interplay of factors that can influence treatment success rates and develop more effective treatment strategies for infertile couples. Further research is needed to fully understand the impact of various parameters on disease control and to optimize treatment approaches for couples with different degrees of oligospermia.

The second model proposed for male infertility incorporates essential details, introducing a more comprehensive framework that includes sperm sampling methods in infertile couples. A baseline examination for sperm collection in cases of severe male factor infertility involves semen analysis, which is the first test to obtain in a couple presenting with infertility. The decision between TESE and micro-TESE is critical to the outcome of treatment in cases of severe male factor infertility. According to research, males with severe male factor infertility may benefit more from micro-TESE. However, a reproductive doctor should be consulted before deciding between TESE and micro-TESE based on the unique characteristics of each patient. To properly prove the superiority of micro-TESE over TESE in the context of severe male factor infertility and ICSI treatment, more investigation and clinical data are required⁴⁷. According to a research study comparing micro-TESE and TESE for severe male factor infertility, patients who underwent TESE obtained better results than those who underwent micro-TESE, and more couples conceived. The second group experienced a higher rate of transition from infertile couples to those receiving ICSI treatment and micro-TESE testicular biopsy than the first group. This suggests that the surgical method used for sperm retrieval in cases of severe male factor infertility is essential to the therapeutic outcome^{48–50}. The results suggest that micro-TESE might be a good choice for sperm retrieval in cases of severe male factor, especially if ICSI is being explored. However, a reproductive doctor should be consulted before deciding between TESE and micro-TESE based on the unique characteristics of each patient. To properly prove the superiority of micro-TESE over TESE in the context of severe oligospermia and ICSI treatment, more investigation and clinical data are required. The variables influencing the success rate of micro-TESE and TESE in cases of severe male factor infertility require further study. This could aid in the creation of more effective treatment plans for couples whose infertility is caused by this particular issue.

The predicted evolution of infertile couples with both male factor and severe male factor infertility, considering different sperm sampling methods, showed that the turquoise blue graph in Figs. 5–910 demonstrates an increase in the first group and relative constancy in the second group. This indicates a higher treatment rate for the first

group. Also, in analyzing the ICSI method (Fig. 9 and Fig. 10), the first group initially has a higher rate, but the second group catches up, eventually surpassing the first group. This emphasizes that treatment method selection and its outcomes occur more rapidly in the second group.

Limitations

The dynamical models for male infertility presented in this article show promise but are subject to specific limitations. Male infertility is a highly complex disorder with a wide range of presentations among infertile men. This complexity arises from the dynamic transcription of approximately 4000 genes in different subtypes of germ cells during human spermatogenesis. The intricate nature of these models can restrict their ability to make accurate predictions. Furthermore, the models are based on the current understanding of male infertility and require further refinement to improve their predictive capabilities. Infertility is an evolving field of study. For instance, the cause of infertility remains unknown in approximately 40% of infertile men, and identifying new genetic variables associated with unexplained male infertility is a major focus of current research⁵¹. Consequently, the models presented may not fully account for all the factors contributing to male infertility. Additionally, the implementation of these models in clinical settings has been limited due to a lack of confidence in their efficacy and challenges in integrating them into clinical protocols⁵². This study emphasizes theoretical modeling and sensitivity analysis; however, we acknowledge that validation using real-world clinical data is essential to assess the models' reliability. The credibility of our approach would be significantly enhanced by directly comparing model predictions with observed ART success rates across diverse data sets. To improve model accuracy and predictive performance, future research should aim to incorporate clinical data into the modeling process. It is also important to recognize several potential limitations. First, accurate model calibration depends on the availability of high-quality, individualized clinical data, which may not always be accessible. Second, inherent biological variability among patients can limit the generalizability of the model's outcomes. Finally, integrating such models into routine clinical practice presents challenges related to interpretability, user acceptance, and regulatory approval. Addressing these challenges will be essential for translating theoretical models into practical tools in reproductive medicine.

Future directions

Future research into male infertility could benefit from adopting a multi-omics approach, which integrates genomics, transcriptomics, proteomics, and metabolomics. This comprehensive method would offer a deeper understanding of the treatment process⁵³, potentially improving the accuracy of dynamic models and facilitating the identification of new biomarkers and treatments for male infertility.

Our current models utilize clinical and laboratory parameters to estimate ART success rates. However, integrating genetic markers associated with sperm function and quality could enable more precise stratification of patient subgroups. In the current modeling framework, transitions between infertility states (e.g., untreated, undergoing IUI, IVF, or ICSI) are primarily driven by empirical treatment success rates (see^{54–57}). For instance, the identification of genetic variants linked to infertility through genomic analyses could facilitate the classification of couples into subgroups with distinct treatment pathways and success probabilities. Similarly, characterizing sperm metabolic profiles may enhance the prediction of ART outcomes and support the development of personalized treatment strategies⁵⁴. Moreover, the analysis of sperm ribonucleic acid (RNA) and protein expression can offer insights into sperm quality and fertilization potential, which may help refine key model parameters such as δ_1 , δ_2 , and δ_3 .

Furthermore, developing more tailored models specific to local populations could enhance the prognosis-based strategy for unexplained infertility⁵². Future research should focus on identifying new genetic variables associated with idiopathic male infertility⁵¹. For instance, male infertility is often influenced by genetic abnormalities, such as Y-chromosome microdeletions, chromosomal rearrangements, and single-gene mutations⁵⁸. These factors can significantly impact sperm production, motility, and fertilization potential. Incorporating genetic data into the SITR models enables more refined classification of infertile couples and enhances the accuracy of treatment outcome predictions. For example, couples with specific microdeletions may exhibit lower success rates with conventional IVF and might require ICSI as a first-line treatment. This can be modeled by adjusting the transition probabilities (η_2 and η_3) in the treatment equations. Moreover, gene mutations can influence the selection of sperm retrieval techniques, which can be reflected in parameters K_2 and K_3 ⁵⁹. By incorporating genetic predispositions as weighting factors in these transition rates, the models may provide more personalized and biologically informed predictions. For example, patients with protamine-1 and protamine-2 deficiencies, which are known to affect sperm chromatin packaging may exhibit altered probabilities of success with ICSI. These genetic effects can be quantitatively integrated into the bifurcation analysis of the proposed models (see^{60,61}).

Similarly, hormonal factors such as low testosterone or elevated follicle stimulating hormone (FSH) levels are commonly observed in men with infertility⁶². These factors can influence both sperm production and the response to ART treatments. By incorporating hormonal profiles into the SITR model, the recovery rates (r_1 and r_2) can be adjusted based on individual hormonal status. For instance, men with normal testosterone levels may experience higher IVF success rates compared to those with hormonal deficiencies. The integration of genetic, hormonal, and multi-omics data into the SITR framework offers several clinical applications, including personalized treatment planning, predictive modeling, and resource allocation. Incorporating these advanced methodologies may enable the SITR models to evolve into powerful tools for understanding and addressing the multifactorial nature of infertility. By treating hormonal levels as dynamic variables rather than static parameters, it becomes possible to introduce feedback mechanisms in which hormonal fluctuations actively influence the probability of ART success over time.

From a computational standpoint, the models can be extended to incorporate multi-omics-informed transition rates, allowing for real-time adaptations based on patient-specific biological profiles. Furthermore, integrating machine learning techniques with the mathematical models may assist in determining optimal threshold values for these biomarkers, thereby enhancing clinical decision-making. Future research should focus on extending the dynamical framework by incorporating these biological insights, ensuring that the models remain clinically relevant and adaptable to emerging infertility diagnostics. Finally, it is essential to work toward increasing the adoption of these models in clinical practice by fostering trust in their efficacy and overcoming the practical obstacles associated with their implementation.

Conclusion

In the present research, two new dynamic models for infertility of couples with men's factors were presented. In the first model, the study population is divided into six groups: infertile susceptible couples, infertile men, couples under IUI treatment, couples receiving in vitro fertilization treatment, men taking ICSI treatment, and recovered couples. In the second model, sperm sampling of infertile couples is also considered. The advantage of the second model over the first model is that sperm sampling is considered. In the second model, the effects and type of sperm sample obtained in recovery and the type of treatment were investigated in more detail. Infertile couples who have Oligospermia infertility and whose sperm sample was obtained by ejaculation use IVF (ICSI) treatment almost 1.5 (28) times more than those with severe Oligospermia.

A basic reproduction number was determined. It was proved that the disease-free equilibrium point for the model is locally stable but not asymptotically stable. It was also shown that the equilibrium point does not have a sign stable. Therefore, the return of diseases disappears, and nonpregnancy and failure in all kinds of treatment no longer remain in the infertile society. Finally, the model was presented graphically. The main achievement of this study is that in the case where oligospermia patients under treatment end up with the treatment T_3 , they will remain in this state. Examining the sensitivity index in the first and second models showed that if the return rate of infertile couples increases, abortions increase, and fewer couples become fertile, then disease control becomes difficult.

In conclusion, while the dynamical models for male infertility present a significant advancement in the field, there is still much work to be done. Future research should aim to address the limitations of these models and explore new methodologies and approaches to improve their predictive power and clinical applicability.

Data and materials availability

The data sets analyzed during the current study are not publicly available due to privacy and legal restrictions, but they may be obtained from the corresponding author upon reasonable request and subject to institutional approval.

Appendix A

Definition 1 ⁶³ The Routh Hurwitz stability criterion expresses that a system having a characteristic equation as follows:

$$P_n(\lambda) = a_0\lambda^n + a_1\lambda^{n-1} + \dots + a_{n-1}\lambda + a_n,$$

the matrix

$$H_n = \begin{pmatrix} a_1 & a_0 & 0 & 0 & 0 & 0 & \dots & 0 \\ a_3 & a_2 & a_1 & a_0 & 0 & 0 & \dots & 0 \\ a_5 & a_4 & a_3 & a_2 & a_1 & a_0 & \dots & 0 \\ \vdots & \vdots & \vdots & \vdots & \vdots & \vdots & \ddots & \vdots \\ 0 & 0 & 0 & 0 & 0 & 0 & \dots & a_n \end{pmatrix}$$

is named the Hurwitz matrix, associated with $P_n(\lambda)$.

The main diagonal of the matrix contains elements a_1, a_2, \dots, a_n . The first column contains numbers with odd indices a_1, a_3, a_5, \dots . In each row, the index of each following number (counting from left to right) is less than the index of its predecessor. All other coefficients with indices greater than n or less than 0 are replaced by zeros. To be asymptotically stable of system, all the principal minors of the H_n must be positive, where the principle minors are as follows:

$$\begin{aligned} \Delta_1 &= |a_1|, \\ \Delta_2 &= \begin{vmatrix} a_1 & a_0 \\ a_3 & a_2 \end{vmatrix}, \\ \Delta_3 &= \begin{vmatrix} a_1 & a_0 & 0 \\ a_3 & a_2 & a_1 \\ a_5 & a_4 & a_3 \end{vmatrix}, \\ &\vdots \\ \Delta_n &= |H_n|. \end{aligned}$$

Liénard and Chipart⁶⁴ demonstrated that if all the coefficients in the characteristic equation are positive ($a_i > 0$ for $i = 1, \dots, n$), then the system is asymptotically stable if either

a) $\Delta_1 > 0, \Delta_3 > 0, \dots$ or

b) $\Delta_2 > 0, \Delta_4 > 0, \dots$. In the following, a theory is described that can not only determine the local stability of the non-hyperbolic equilibrium, but also settle the question of the existence of another equilibrium (bifurcated from the non-hyperbolic equilibrium). Below proposition of Chavez and Song⁶⁵ refers to it.

Proposition 1 Consider a general system of ordinary differential equations with a parameter ϕ as follows:

$$\begin{aligned} \frac{dX}{dt} &= F(X, \phi), \\ F : R^n \times R &\longrightarrow R^n, \\ F &\in C^2(R^n \times R). \end{aligned} \quad (7)$$

Now, consider the following assumptions:

- B is the linearization matrix of System (7) nearby the equilibrium 0 with ϕ evaluated at 0. Zero is a simple eigenvalue of B , and all other eigenvalues of B have negative real parts.
- Matrix B has a nonnegative right eigenvector r and a left eigenvector l corresponding to the zero eigenvalue. Let F_k be the k th component of F and let

$$a = \sum_{k,i,j=1}^n l_k r_i r_j \frac{\partial^2 F_k}{\partial x_i \partial x_j}(0, 0), \quad (8)$$

$$b = \sum_{k,i=1}^n l_k r_i \frac{\partial^2 F_k}{\partial x_i \partial \phi}(0, 0). \quad (9)$$

The local dynamics of system (7) around the equilibrium 0 are totally determined by the constants of a and b as follows:

- $a > 0, b > 0$. When $\phi < 0$ with $|\phi| \ll 1$, 0 is locally asymptotically stable, and there exists a positive unstable equilibrium; when $0 < |\phi| \ll 1$, 0 is unstable and there exists a negative and locally asymptotically stable equilibrium.
- $a < 0, b < 0$. When $\phi < 0$ with $|\phi| \ll 1$, 0 is unstable; when $0 < |\phi| \ll 1$, 0 is locally asymptotically stable, and there exists a positive unstable equilibrium;
- $a > 0, b < 0$. When $\phi < 0$ with $|\phi| \ll 1$, 0 is unstable, and there exists a locally asymptotically stable negative equilibrium; when $0 < |\phi| \ll 1$, 0 is stable, and a positive unstable equilibrium appears;
- $a < 0, b > 0$. When ϕ changes from negative to positive, 0 changes its stability from stable to unstable. Correspondingly a negative unstable equilibrium becomes positive and locally asymptotically stable.

Appendix B

The Constants of characteristic equation of matrix J_{C0} in Theorem 3.

$$b_1 = b_{22} + b_{33} + b_{44} + b_{55} + b_{66} + b_{77},$$

$$\begin{aligned} b_2 = & b_{22}(b_{33} + b_{44} + b_{55} + b_{66} + b_{77}) \\ & + b_{33}(b_{44} + b_{55} + b_{66} + b_{77}) + b_{44}(b_{55} + b_{66} + b_{77}) \\ & + b_{55}(b_{66} + b_{77}) + b_{66}b_{77}, \end{aligned}$$

$$\begin{aligned} b_3 = & -S_0\beta(\delta_1\eta_1\nu_1 + \delta_2\eta_2\nu_1 + \delta_2\eta_4\nu_2 + \delta_2\eta_6\nu_3) \\ & + b_{22}b_{33}(b_{44} + b_{55} + b_{66} + b_{77}) \\ & + b_{22}b_{44}(b_{55} + b_{66} + b_{77}) \\ & + b_{22}b_{55}(b_{66} + b_{77}) \\ & + b_{22}b_{66}b_{77} + b_{33}b_{44}(b_{55} + b_{66} + b_{77}) \\ & + b_{33}b_{55}(b_{66} + b_{77}) + b_{33}b_{66}b_{77} + b_{44}b_{55}(b_{66} + b_{77}) \\ & + b_{44}b_{66}b_{77} + b_{55}b_{66}b_{77}, \end{aligned}$$

$$\begin{aligned} b_4 = & -S_0\beta(hk\delta_1\delta_2\eta_1\nu_1 + b_{33}\delta_2\eta_4\nu_2 + b_{33}\delta_2\eta_6\nu_3 \\ & + b_{44}\delta_1\eta_1\nu_1 + b_{44}\delta_2\eta_2\nu_1 + b_{44}\delta_2\eta_6\nu_3 + b_{55}\delta_1\eta_1\nu_1 \\ & + b_{55}\delta_2\eta_2\nu_1 + b_{55}\delta_2\eta_4\nu_2 + b_{66}\delta_2\eta_2\nu_1 + b_{66}\delta_2\eta_4\nu_2 \\ & + b_{66}\delta_2\eta_6\nu_3 + b_{77}\delta_1\eta_1\nu_1) \\ & + b_{22}b_{33}b_{44}(b_{55} + b_{66} + b_{77}) + b_{22}b_{33}b_{55}(b_{66} + b_{77}) \\ & + b_{22}b_{33}b_{66}b_{77} + b_{22}b_{44}b_{55}(b_{66} + b_{77}) \\ & + b_{22}b_{44}b_{66}b_{77} + b_{22}b_{55}b_{66}b_{77} + b_{33}b_{44}b_{55}(b_{66} + b_{77}) \\ & + b_{33}b_{44}b_{66}b_{77} + b_{33}b_{55}b_{66}b_{77} + b_{44}b_{55}b_{66}b_{77}, \end{aligned}$$

$$\begin{aligned} b_5 = & -S_0\beta(hkb_{44}\delta_1\delta_2\eta_1\nu_1 + hkb_{55}\delta_1\delta_2\eta_1\nu_1 \\ & + b_{33}b_{44}\delta_2\eta_6\nu_3 + b_{33}b_{55}\delta_2\eta_4\nu_2 + b_{33}b_{66}\delta_2\eta_4\nu_2 \\ & + b_{33}b_{66}\delta_2\eta_6\nu_3 + b_{44}b_{55}\delta_1\eta_1\nu_1 + b_{44}b_{55}\delta_2\eta_2\nu_1 \\ & + b_{44}b_{66}\delta_2\eta_2\nu_1 + b_{44}b_{66}\delta_2\eta_6\nu_3 + b_{44}b_{77}\delta_1\eta_1\nu_1 \\ & + b_{55}b_{66}\delta_2\eta_2\nu_1 + b_{55}b_{66}\delta_2\eta_4\nu_2 + b_{55}b_{77}\delta_1\eta_1\nu_1) \\ & + b_{22}b_{33}b_{44}b_{55}(b_{66} + b_{77}) + b_{22}b_{33}b_{44}b_{66}b_{77} \\ & + b_{22}b_{33}b_{55}b_{66}b_{77} + b_{22}b_{44}b_{55}b_{66}b_{77} \\ & + b_{33}b_{44}b_{55}b_{66}b_{77}, \end{aligned}$$

$$b_6 = (1 - R_{C0})b_{22}b_{33}b_{44}b_{55}b_{66}b_{77}.$$

Appendix C

The components of endemic equilibrium point E^{C*} .

$$s^{C*} = \frac{S_0}{R_{C0}}, \quad K_1^{C*} = \frac{\nu_1 I^{C*}}{b_{22}},$$

$$K_2^{C*} = \frac{\nu_2 I^{C*}}{b_{44}}, \quad K_3^{C*} = \frac{\nu_3 I^{C*}}{b_{55}},$$

$$T_1^{C*} = \frac{\nu_1 \eta_1 I^{C*}}{b_{33} b_{66}},$$

$$T_2^{C*} = \left(\frac{b_{22} I^{C*}}{\beta \delta_2 s_0} \right) \left(R_{C0} - \frac{\beta}{\delta_1} \eta_1 s_0 \nu_1 b_{22} b_{33} b_{66} \right),$$

$$T_3^{C*} = \left(\frac{I^{C*}}{\delta_3 + \alpha} \right) \left(\frac{\nu_1 \eta_3}{b_{33}} + \frac{\nu_2 \eta_5}{b_{44}} + \frac{\nu_3 \eta_7}{b_{55}} \right. \\ \left. + \nu_2 \delta_2 T_2^{C*} + \frac{(1-k) h \delta_1 \nu_1 \eta_1}{b_{33} b_{66}} \right),$$

$$I^{C*} = \frac{L R_{C0} - \alpha S_0}{b_{22}},$$

Appendix D

The Constants of characteristic equation of matrix $J(E^{C*}, \beta^*)$ in Theorem 4.

$$p_1 = b_{22} + b_{33} + b_{44} + b_{55} + b_{66} + b_{77},$$

$$p_2 = b_{22}(b_{33} + b_{44} + b_{55} + b_{66} + b_{77}) \\ + b_{33}(b_{44} + b_{55} + b_{66} + b_{77}) \\ + b_{44}(b_{55} + b_{66} + b_{77}) + b_{55}(b_{66} + b_{77}) + b_{66}b_{77},$$

$$p_3 = -S_0 \beta (\delta_1 \eta_1 v_1 + \delta_2 \eta_2 v_1 + \delta_2 \eta_4 v_2 + \delta_2 \eta_6 v_3) \\ + b_{22} b_{33} (b_{44} + b_{55} + b_{66} + b_{77}) \\ + b_{22} b_{44} (b_{55} + b_{66} + b_{77}) + b_{22} b_{55} (b_{66} + b_{77}) \\ + b_{22} b_{66} b_{77} + b_{33} b_{44} (b_{55} + b_{66} + b_{77}) \\ + b_{33} b_{55} (b_{66} + b_{77}) + b_{33} b_{66} b_{77} + b_{44} b_{55} (b_{66} + b_{77}) \\ + b_{44} b_{66} b_{77} + b_{55} b_{66} b_{77},$$

$$p_4 = -S_0 \beta (h k \delta_1 \delta_2 \eta_1 v_1 + b_{33} \delta_2 \eta_4 v_2 + b_{33} \delta_2 \eta_6 v_3 \\ + b_{44} \delta_1 \eta_1 v_1 + b_{44} \delta_2 \eta_2 v_1 + b_{44} \delta_2 \eta_6 v_3 + b_{55} \delta_1 \eta_1 v_1 \\ + b_{55} \delta_2 \eta_2 v_1 + b_{55} \delta_2 \eta_4 v_2 + b_{66} \delta_2 \eta_2 v_1 + b_{66} \delta_2 \eta_4 v_2 \\ + b_{66} \delta_2 \eta_6 v_3 + b_{77} \delta_1 \eta_1 v_1) \\ + b_{22} b_{33} b_{44} (b_{55} + b_{66} + b_{77}) + b_{22} b_{33} b_{55} (b_{66} + b_{77}) \\ + b_{22} b_{33} b_{66} b_{77} + b_{22} b_{44} b_{55} (b_{66} + b_{77}) + b_{22} b_{44} b_{66} b_{77} \\ + b_{22} b_{55} b_{66} b_{77} + b_{33} b_{44} b_{55} (b_{66} + b_{77}) \\ + b_{33} b_{44} b_{66} b_{77} + b_{33} b_{55} b_{66} b_{77} + b_{44} b_{55} b_{66} b_{77},$$

$$p_5 = -S_0 \beta (h k b_{44} \delta_1 \delta_2 \eta_1 v_1 + h k b_{55} \delta_1 \delta_2 \eta_1 v_1 \\ + b_{33} b_{44} \delta_2 \eta_6 v_3 + b_{33} b_{55} \delta_2 \eta_4 v_2 + b_{33} b_{66} \delta_2 \eta_4 v_2 \\ + b_{33} b_{66} \delta_2 \eta_6 v_3 + b_{44} b_{55} \delta_1 \eta_1 v_1 + b_{44} b_{55} \delta_2 \eta_2 v_1 \\ + b_{44} b_{66} \delta_2 \eta_2 v_1 + b_{44} b_{66} \delta_2 \eta_6 v_3 + b_{44} b_{77} \delta_1 \eta_1 v_1 \\ + b_{55} b_{66} \delta_2 \eta_2 v_1 + b_{55} b_{66} \delta_2 \eta_4 v_2 + b_{55} b_{77} \delta_1 \eta_1 v_1) \\ + b_{22} b_{33} b_{44} b_{55} (b_{66} + b_{77}) + b_{22} b_{33} b_{44} b_{66} b_{77} \\ + b_{22} b_{33} b_{55} b_{66} b_{77} + b_{22} b_{44} b_{55} b_{66} b_{77} \\ + b_{33} b_{44} b_{55} b_{66} b_{77}.$$

Received: 5 December 2024; Accepted: 23 May 2025

Published online: 29 May 2025

References

1. Murray, J. D. *Mathematical biology II: spatial models and biomedical applications* (Springer, New York, 2001).
2. Boccia, E., Luther, S. & Parltitz, U. Modelling far field pacing for terminating spiral waves pinned to ischaemic heterogeneities in cardiac tissue. *Phil. Trans. R. Soc. A* **375**(2096), 20160289 (2017).
3. Bozkurt, F., Yousef, A. & Abdeljawad, T. Analysis of the outbreak of the novel coronavirus COVID-19 dynamic model with control mechanisms. *Results Phys.* **19**, 103586 (2020).
4. Ghiasihafezi, S., Ahmadizand, M. R. & Molaei, M. A dynamical model for the number of infertile couples. *Health Inf. Sci. Syst.* **6**, 1–9 (2018).
5. Giordano, G. et al. Modelling the COVID-19 epidemic and implementation of population-wide interventions in Italy. *Nat. Med.* **26**, 855–860 (2020).
6. Grossman, Z. & Herberman, R. Mathematical models of HIV pathogenesis. *Nat. Med.* **3**, 936–937 (1997).
7. Owen, B. N. et al. Dynamical malaria modeling as a tool for bold policy-making. *Nat. Med.* **28**, 610–611 (2022).
8. Singh, H., Srivastava, H. M. & Baleanu, D. *Methods of Mathematical Modeling* (Academic Press, Infectious Diseases, 2022).
9. Ross, R. An application of the theory of probabilities to the study of a priori pathometry Part I. In: *Proceedings of the Royal Society of London. Series A. Containing Papers of a Mathematical and Physical Character.* **92**(638), 204–230 (1916).
10. Ross, R. & Hudson, H. An application of the theory of probabilities to the study of a priori pathometry. Part II. In: *Proceedings of the Royal Society of London. Series A, Containing Papers of a Mathematical and Physical Character.* **93**(650), 212–225 (1917).
11. Ross, R. & Hudson, H. An application of the theory of probabilities to the study of a priori pathometry. Part III. In: *Proceedings of the Royal Society of London. Series A, Containing Papers of a Mathematical and Physical Character.* **89**(621), 225–240 (1917).
12. Kermack, W. O. & McKendrick, A. G. A contribution to the mathematical theory of epidemics. *Proceedings of the Royal Society of London. Series A, Containing Papers of a Mathematical and Physical Character.* **115**(700), 700–721 (1927).
13. Kendall, D. G. Deterministic and stochastic epidemics in closed populations. *Proceedings of the Third Berkeley Symposium on Mathematical Statistics and Probability: Contributions to Biology and Problems of Health.* **4**, 149–165 (1956).
14. Agarwal, A., Mulgund, A., Hamada, A. & Chyatte, M. R. A unique view on male infertility around the globe. *Reprod. Biol. Endocrinol.* **13**(1), 1–9 (2015).
15. Chau, M. H. K. et al. Investigation of the genetic etiology in male infertility with apparently balanced chromosomal structural rearrangements by genome sequencing. *Asian J. Androl.* **24**(3), 248–254 (2022).
16. Barati, E., Nikzad, H. & Karimian, M. Oxidative stress and male infertility: Current knowledge of pathophysiology and role of antioxidant therapy in disease management. *Cell. Mol. Life Sci.* **77**, 93–113 (2020).
17. Ilacqua, A., Izzo, G., Pietro Emerenziani, G., Baldari, C. & Aversa, A. Lifestyle and fertility: the influence of stress and quality of life on male fertility. *Reprod. Biol. Endocrinol.* **16**, 1–11 (2018).
18. Agarwal, A. et al. Male infertility. *Lancet.* **397**(10271), 319–333 (2021).
19. WHO laboratory manual for the examination and processing of human semen, sixth edition. Geneva: World Health Organization; 2021. Licence: CC BY-NC-SA 3.0 IGO.
20. Jedrzejczak, P., Taszarek-Hauke, G., Hauke, J., Pawelczyk, L. & Duleba, A. J. Prediction of spontaneous conception based on semen parameters. *Int. J. Androl.* **31**, 499–507 (2008).
21. Schlegel, P. N. et al. Diagnosis and treatment of infertility in men: AUA/ASRM guideline part I. *Fertil. Steril.* **115**(1), 54–61 (2021).
22. Baskaran, S., Finelli, R., Agarwal, A. & Henkel, R. Diagnostic value of routine semen analysis in clinical andrology. *Andrologia* **53**(2), e13614 (2020).
23. Sharma, A., Minhas, S., Dhillon, W. S. & Jayasena, C. N. Male infertility due to testicular disorders. *J. Clin. Endocrinol. Metab.* **106**(2), 442–459 (2021).
24. Dicke, A. K. et al. DDX3Y is likely the key spermatogenic factor in the AZFa region that contributes to human non-obstructive azoospermia. *Commun. Biol.* **6**(1), 350 (2023).
25. Jin, H. J. et al. CFAP70 is a solid and valuable target for the genetic diagnosis of oligo-astheno-teratozoospermia in infertile men. *EBioMedicine.* **93**, 104675 (2023).
26. Ogawa, T. et al. Transplantation of male germ line stem cells restores fertility in infertile mice. *Nat. Med.* **6**, 29–34 (2000).
27. Boivin, J., Bunting, L., Collins, J. A. & Nygren, K. G. International estimates of infertility prevalence and treatment-seeking: potential need and demand for infertility medical care. *Hum. Reprod.* **22**(6), 1506–1512 (2007).
28. Dubin, J. M. et al. Men With Severe Oligospermia Appear to Benefit From Varicocele Repair: A Cost-effectiveness Analysis of Assisted Reproductive Technology. *Urology.* **111**, 99–103 (2018).
29. Ferlin, A. et al. Management of male factor infertility: position statement from the Italian Society of Andrology and Sexual Medicine (SIAMS): Endorsing Organization: Italian Society of Embryology, Reproduction, and Research (SIERR). *J. Endocrinol. Invest.* **45**(5), 1085–1113 (2022).
30. Calhaz-Jorge, C. et al. Assisted reproductive technology in Europe, 2012: results generated from European registers by ESHRE. *Hum. Reprod.* **31**(8), 1638–1652 (2016).
31. Ombelet, W., Dhont, N., Thijssen, A., Bosmans, E. & Kruger, T. Semen quality and prediction of IUI success in male subfertility: a systematic review. *Reprod. Biomed. Online.* **28**(3), 300–309 (2014).
32. Katzorke, T. & Kolodziej, F. B. The significance of insemination in the era of IVF and ICSI. *Urology.* **49**(7), 842–846 (2010).
33. Tournaye, H. et al. Intracytoplasmic sperm injection versus in vitro fertilization: a randomized controlled trial and a meta-analysis of the literature. *Fertil. Steril.* **78**(5), 1030–1037 (2002).
34. Santi, D. et al. Which sperm parameter limits could really guide the clinical decision in assisted reproduction. *Andrology.* **11**(1), 143–154 (2023).
35. Mazzilli, R. et al. Effect of the male factor on the clinical outcome of intracytoplasmic sperm injection combined with preimplantation aneuploidy testing: observational longitudinal cohort study of 1,219 consecutive cycles. *Fertil. Steril.* **108**(6), 961–972 (2017).
36. Mazzilli, R. et al. Male factor infertility and assisted reproductive technologies: indications, minimum access criteria and outcomes. *J. Endocrinol. Invest.* **46**(6), 1079–1085 (2023).
37. Pelinck, M. J., Hoek, A., Simons, A. H. M. & Heineman, M. J. Efficacy of natural cycle IVF: a review of the literature. *Hum. Reprod. Update.* **8**(2), 129–139 (2002).
38. Sharma, R., Biedenharn, K. R., Fedor, J. M. & Agarwal, A. Lifestyle factors and reproductive health: taking control of your fertility. *Reprod. Biol. Endocrinol.* **11**, 1–15 (2013).
39. Sundaram, R., Mumford, S. L. & Buck Louis, G. M. Couples' body composition and time-to-pregnancy. *Hum. Reprod.* **32**(3), 662–668 (2017).
40. Hanson, B. et al. Female infertility, infertility-associated diagnoses, and comorbidities: a review. *J. Assist. Reprod. Genet.* **33**(2), 127–136 (2016).
41. Zegers-Hochschild, F. et al. The International Glossary on Infertility and Fertility Care. *Hum. Reprod.* **32**(9), 1786–1801 (2017).
42. Cohlen, B. J., Vandekerckhove, P., te Velde, E. R., & Habbema, J. D. F. Timed intercourse versus intra-uterine insemination with or without ovarian hyperstimulation for subfertility in men. *Cochrane Database Syst. Rev.*, (2) CD000360 (2000).

43. Diekmann, O., Heesterbeek, J. A. P. & Metz, J. A. J. On the definition and computation of the basic reproduction ratio \mathcal{R}_0 in models for infectious diseases in heterogeneous populations. *J. Math. Biol.* **28**(4), 356–382 (1990).
44. Catalini, L., Fedder, J., Nørgard, B. M. & Jølvig, L. R. Assisted Reproductive Technology Results Using Donor or Partner Sperm: A Danish Nationwide Register-Based Cohort Study. *J. Clin. Med.* **12**(7), 2571 (2023).
45. Alharbi, M., Almarzouq, A. & Zini, A. Sperm retrieval and intracytoplasmic sperm injection outcomes with testicular sperm aspiration in men with severe oligozoospermia and cryptozoospermia. *Can. Urol. Assoc. J.* **15**(5), E272 (2020).
46. Li, L. & Zhao, S. Outcome analysis of ICSI assisted pregnancy using testicular sperm versus ejaculated sperm in man with severe oligozoospermia in the same ART cycle: A case report. *Medicine* **102**(5), e32833 (2023).
47. Najari, B. B. Varicocele Repair in Men With Severe Oligospermia: NYU Case of the Month. *Rev. Urol.* **21**(1), 32–34 (2019).
48. Alkandari, M. H., Moryousef, J., Phillips, S. & Zini, A. Testicular Sperm Aspiration (TESA) or Microdissection Testicular Sperm Extraction (Micro-tese): Which Approach is better in Men with Cryptozoospermia and Severe Oligozoospermia?. *Urology* **154**, 164–169 (2021).
49. Esteves, S. C. Microdissection TESE versus conventional TESE for men with nonobstructive azoospermia undergoing sperm retrieval. *Int. Braz. J. Urol.* **48**(3), 569–578 (2022).
50. Vahidi, S. et al. Success rate and ART outcome of microsurgical sperm extraction in non obstructive azoospermia: A retrospective study. *Int. J. Reprod. Biomed.* **19**(9), 781–788 (2021).
51. Sudhakar, D. V. S., Shah, R. & Gajbhiye, R. K. Genetics of Male Infertility - Present and Future: A Narrative Review. *J. Hum. Reprod. Sci.* **14**(3), 217–227 (2021).
52. Shingshetty, L., Maheshwari, A., McLernon, D. J. & Bhattacharya, S. Should we adopt a prognosis-based approach to unexplained infertility? *Hum. Reprod. Open.* **2022**(4), hoac046 (2022).
53. Wagner, A. O., Turk, A. & Kunej, T. Towards a Multi-Omics of Male Infertility. *World J. Mens Health.* **41**(2), 272–288 (2023).
54. Amaral, A., Paiva, C. & Baptista, M. Sperm metabolism and fertility: A review. *Reprod. Biol. Endocrinol.* **11**(1), 1–10 (2013).
55. Espinel-Rios, S., Lopez, J. M. & Avalos, J. L. Omics-driven hybrid dynamic modeling of bioprocesses with uncertainty estimation. *Biochemical Engineering Journal* **216**, 109637 (2025).
56. Huang, S. et al. Multionics identification of programmed cell death-related characteristics for nonobstructive azoospermia based on a 675-combination machine learning computational framework. *Genomics* **117**(1), 110977 (2025).
57. Sengupta, P. et al. Reproductomics: Exploring the Applications and Advancements of Computational Tools. *Physiol. Res.* **73**(5), 687–702 (2024).
58. Krausz, C. & Hoefsloot, L. EAA/EMQN best practice guidelines for molecular diagnosis of Y-chromosomal microdeletions: State-of-the-art. *Andrology* **2**(1), 5–19 (2014).
59. Krausz, C. & Riera-Escamilla, A. Genetics of male infertility. *Nat. Rev. Urol.* **15**(6), 369–384 (2018).
60. Bibi, R. et al. Protamines and DNA integrity as a biomarkers of sperm quality and assisted conception outcome. *Andrologia* **54**(6), e14418 (2022).
61. Ejaz, H., Arshad, A., Irfan, M., Ismail, S. B., & Hussain, N. H. N. Association of Single Nucleotide Polymorphisms (rs2301365 & Rs737008) in PRM1 Gene and Male Infertility: A Meta-Analysis. *J. Sex. Med.* **21**(2), qdae002–215 (2024).
62. Dohle, G. R. et al. Guía clínica sobre la infertilidad masculina. *European Association of Urology* 1–69 (2010).
63. Roskilly, T. & Mikalsen, R. *Marine Systems Identification* (Butterworth-Heinemann, Modeling and Control, 2015).
64. Lienard, A. & Chipart, M. H. Sur le signe de la partie réelle des racines d'une equation algebrique. *J. Math. Pures Appl.* **10**(6), 291–346 (1914).
65. Castillo-Chavez, C. & Song, B. Dynamical Models of Tuberculosis and Their Applications. *Math. Biosci. Eng.* **1**, 361–404 (2004).

Author contributions

S. Ghiasi Hafazi and M. Ranjbar wrote the original draft and methodology. A. Ghasemabadi prepared formal analysis. S. Effati do supervision and validation. A. Naserghandi, K. Namakin and F. Allameh prepared conceptualization. All authors reviewed the manuscript.

Funding

This research did not receive any specific grant from funding agencies in the public, commercial, or not-for-profit sectors.

Declarations

Competing interests

The authors declare no competing interests.

Ethical approval

The study involving human participants was reviewed and approved by the Ethics Committee of Yazd University (Approval Number: IR.YAZD.REC.1401.019).

Additional information

Correspondence and requests for materials should be addressed to M.R. or S.E.

Reprints and permissions information is available at www.nature.com/reprints.

Publisher's note Springer Nature remains neutral with regard to jurisdictional claims in published maps and institutional affiliations.

Open Access This article is licensed under a Creative Commons Attribution-NonCommercial-NoDerivatives 4.0 International License, which permits any non-commercial use, sharing, distribution and reproduction in any medium or format, as long as you give appropriate credit to the original author(s) and the source, provide a link to the Creative Commons licence, and indicate if you modified the licensed material. You do not have permission under this licence to share adapted material derived from this article or parts of it. The images or other third party material in this article are included in the article's Creative Commons licence, unless indicated otherwise in a credit line to the material. If material is not included in the article's Creative Commons licence and your intended use is not permitted by statutory regulation or exceeds the permitted use, you will need to obtain permission directly from the copyright holder. To view a copy of this licence, visit <http://creativecommons.org/licenses/by-nc-nd/4.0/>.

© The Author(s) 2025